

Nonlinear Responses of Sloshing in Square Tanks Subjected to Horizontal Random Ground Excitation

T. Ikeda¹, Y. Harata¹, and R. A. Ibrahim²

¹Department of Mechanical Systems Engineering, Hiroshima University, 1-4-1 Kagamiyama, Higashi-Hiroshima, Japan, 739-8527

²Department of Mechanical Engineering, Wayne State University, Detroit, MI, USA, 48202

Abstract. Nonlinear responses of the predominant two sloshing modes in a square tank have been investigated when the tank is subjected to horizontal, narrow-band random ground excitation. Galerkin's method is applied to derive the modal equations of motion for nonlinear sloshing. Then the Monte Carlo simulation is used to calculate the mean square responses of these two modes. These two modes are nonlinearly coupled with each other, known as 'autoparametric interaction'. The responses differ significantly from those of the corresponding linear model, depending on the characteristics of the narrow-band ground excitation such as the bandwidth, center frequency and the intensity. In addition, it is found that the direction of the excitation is a significant factor in predicting the mean square responses.

1 Introduction

Sloshing dynamics is one of the most important issues in mechanical, civil, marine and aeronautical engineering. Housener [1] presented a linear sloshing model to investigate the responses of free surfaces in partially-filled liquid tanks subjected to horizontal, seismic excitation. It is well known that sloshing at large amplitudes exhibits nonlinear behaviour, thus nonlinear models have been developed to obtain more accurate results. A comprehensive book on nonlinear sloshing dynamics was compiled by Ibrahim [2]. Ground-breaking studies on nonlinear sloshing behaviour in cylindrical tanks subjected to horizontal, and/or vertical harmonic excitation were theoretically and experimentally examined by Hutton [3] and Abramson et al. [4]. Three-dimensional sloshing in square tanks subjected to horizontal, harmonic excitation was theoretically investigated and their results were compared with experimental data [5, 6]. Few examples of nonlinear sloshing behaviour under random excitation exist. However, Sakata et al. investigated a cylindrical tank under random base excitation using modal equations of motion for sloshing [7]. Responses of sloshing in a rectangular tank were also investigated using the finite element method [8]. Furthermore, nonlinear responses of elastic structures with cylindrical tanks subjected to vertical random excitation were also investigated [9, 10].

The present paper investigates the system in which the square tank is subjected to horizontal random excitation using the model of reference [6]. Galerkin's

method is employed to derive the nonlinear modal equations of motion for sloshing. These modal equations are solved using the Monte Carlo simulation and the mean square responses of the predominant two sloshing modes are calculated when the liquid tank is subjected to horizontal, narrow-band random excitation. The influences of the bandwidth and center frequency of the random excitation and the deviation angle of the tank are examined.

2 Theoretical analysis

2.1 Equations of motion

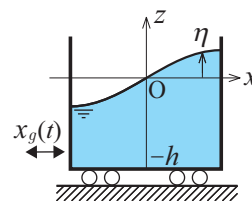
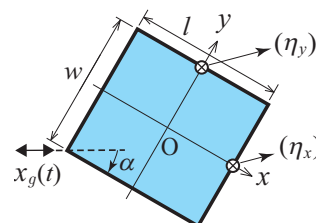
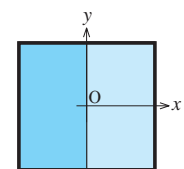
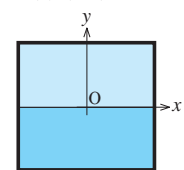


Fig. 1. Theoretical model.



(a) (1,0) mode



(b) (0,1) mode

Fig. 2. Mode shapes.

Figure 1 shows a model for the theoretical analysis. A nearly square tank with length l and breadth w is partially filled with liquid to the level h . The Cartesian coordinate system $O-xyz$ is fixed to the tank where the xy -plane coincides with the undisturbed liquid surface. The tank is horizontally subjected to random ground excitation $x_g(t)$ and the direction of excitation deviates from the tank length by angle α . In the theoretical analysis, the liquid is assumed to be a perfect fluid; hence the velocity potential $\phi(x, y, z, t)$ can be introduced. $P(x, y, z, t)$ is the fluid pressure, ρ is the fluid density, and $\eta(x, y, t)$ is the liquid elevation at position (x, y) in the tank. The following dimensionless quantities are introduced:

$$\left. \begin{aligned} h' &= h/l, w' = w/l, x' = x/l, x'_g = x_g/l, y' = y/l, \\ P' &= P/(\rho l^2 p_{10}^2), z' = z/l, \eta' = \eta/l, \phi' = \phi/(l^2 p_{10}), \\ \lambda'_{ij} &= \lambda_{ij}l, p'_{ij} = p_{ij}/p_{10}, t' = p_{10}t, \end{aligned} \right\} \quad (1)$$

where

$$\lambda_{ij} = \pi \sqrt{(i/l)^2 + (j/w)^2}, \quad p_{ij} = \sqrt{g \lambda_{ij} \tanh(\lambda_{ij} h)}. \quad (2)$$

Here g is the acceleration of gravity and p_{ij} represents the natural frequency of (i, j) sloshing mode. Figures 2(a) and 2(b) show the shapes of $(1, 0)$ and $(0, 1)$ sloshing modes, respectively. Their nodal lines coincide with the y - and x -axes, respectively. All primes “ ’ ” in Eq. (1) will hereafter be omitted for simplicity, although the quantities are still dimensionless in the theoretical analysis and results.

Laplace's equation and Euler's energy equation for the fluid motion are expressed in the dimensionless form, respectively:

$$\frac{\partial^2 \phi}{\partial x^2} + \frac{\partial^2 \phi}{\partial y^2} + \frac{\partial^2 \phi}{\partial z^2} = 0, \quad (3)$$

$$\frac{\partial \phi}{\partial t} + \frac{1}{2} \left[\left(\frac{\partial \phi}{\partial x} \right)^2 + \left(\frac{\partial \phi}{\partial y} \right)^2 + \left(\frac{\partial \phi}{\partial z} \right)^2 \right] + \frac{z}{\psi_{10}} + P = -\ddot{x}_g x \cos \alpha - \ddot{x}_g y \sin \alpha, \quad (4)$$

where $\psi_{10} = \lambda_{10} \tanh(\lambda_{10} h)$. The boundary conditions for the fluid velocity at the tank walls and bottom are:

$$\left. \begin{aligned} \frac{\partial \phi}{\partial x} &= 0 \quad (\text{at } x = \pm 1/2), \quad \frac{\partial \phi}{\partial y} = 0 \quad (\text{at } y = \pm w/2), \\ \frac{\partial \phi}{\partial z} &= 0 \quad (\text{at } z = -h). \end{aligned} \right\} \quad (5)$$

In addition, the kinematic boundary condition at the liquid free surface is:

$$\frac{\partial \phi}{\partial z} = \frac{\partial \eta}{\partial t} + \frac{\partial \phi}{\partial x} \frac{\partial \eta}{\partial x} + \frac{\partial \phi}{\partial y} \frac{\partial \eta}{\partial y} \quad (\text{at } z = \eta). \quad (6)$$

Because $P = 0$ at the liquid free surface, the boundary condition for Eq. (5) is:

$$\frac{\partial \phi}{\partial t} + \frac{1}{2} \left[\left(\frac{\partial \phi}{\partial x} \right)^2 + \left(\frac{\partial \phi}{\partial y} \right)^2 + \left(\frac{\partial \phi}{\partial z} \right)^2 \right] + \frac{z}{\psi_{10}} = -\ddot{x}_g x \cos \alpha - \ddot{x}_g y \sin \alpha \quad (\text{at } z = \eta). \quad (7)$$

The ground excitation $x_g(t)$ is assumed to be generated from the linear shaping filter as follows:

$$\ddot{x}_g + \gamma \dot{x}_g + \Omega^2 x_g = \Omega W(t), \quad (8)$$

where $W(t)$ is a zero-mean stationary Gaussian white noise process with variance σ_w^2 and constant power spectral density intensity S_0 . γ is the bandwidth and Ω is the center frequency. Equations (3) through (8) constitute the boundary value problem of liquid in square and nearly square tanks.

2.2 Modal equations of motion for sloshing

Galerkin's method is used to derive modal equations of motion for sloshing. ϕ and η are assumed in terms of the eigenfunctions which can be obtained from the corresponding linear system, as follows:

$$\phi(x, y, z, t) = \sum_{i=0}^{\infty} \sum_{j=0}^{\infty} a_{ij}(t) U_{ij}(x, y) \cosh\{\lambda_{ij}(z+h)\} / \cosh(\lambda_{ij} h), \quad (9a)$$

$$\eta(x, y, t) = \sum_{i=0}^{\infty} \sum_{j=0}^{\infty} b_{ij}(t) U_{ij}(x, y), \quad (9b)$$

in which $U_{ij}(x, y)$ represent eigenfunctions:

$$U_{ij}(x, y) = \begin{cases} \sin(\lambda_{i0} x) \sin(\lambda_{0j} y) & (i = 2m+1, j = 2n+1) \\ \sin(\lambda_{i0} x) \cos(\lambda_{0j} y) & (i = 2m+1, j = 2n) \\ \cos(\lambda_{i0} x) \sin(\lambda_{0j} y) & (i = 2m, j = 2n+1) \\ \cos(\lambda_{i0} x) \cos(\lambda_{0j} y) & (i = 2m, j = 2n) \end{cases} \quad (10)$$

where m and n are integers. Note that λ_{ij} in Eq. (10) represent dimensionless quantities given by Eqs. (1) and (2). $a_{ij}(t)$ and $b_{ij}(t)$ in Eqs. (9a,b) are unknown functions of time. The coordinates x and y in Eqs. (4) and (7) are expanded in terms of the eigenfunctions of Eq. (10):

$$x = \sum_{i=1}^{\infty} [r_{i0} U_{i0}(x, y)], \quad y = \sum_{j=1}^{\infty} [r_{0j} U_{0j}(x, y)] \quad (11)$$

where the coefficients r_{i0} and r_{0j} are determined by the method used in the previous paper [11]. ε is introduced as a bookkeeping parameter to determine the approximate solutions when two sloshing modes $(1, 0)$ and $(0, 1)$ predominantly appear. Therefore, the orders of $a_{ij}(t)$, $b_{ij}(t)$, x_g , and the system parameters are assumed:

$$\left. \begin{aligned} a_{10}, a_{01}, b_{10}, b_{01}, \zeta_{ij} &\approx O(\varepsilon^{1/3}), \\ a_{20}, a_{02}, a_{30}, a_{03}, a_{11}, b_{20}, b_{02}, b_{30}, b_{03}, b_{11} &\approx O(\varepsilon^{2/3}), \\ a_{i0}, a_{0j}, a_{ij}, b_{i0}, b_{0j}, b_{ij}, x_g &\approx O(\varepsilon^{3/3}) \quad (i \geq 4, j \geq 4). \end{aligned} \right\} \quad (12)$$

Equations (6) and (7) are expanded near $\eta = 0$, and Eqs. (9a,b) are substituted into these two resulting equations. By equating the coefficients of $\sin(\lambda_{i0} x)$, $\sin(\lambda_{0j} y)$,

$\cos(\lambda_{20}x)$, $\cos(\lambda_{02}y)$, $\sin(\lambda_{30}x)$, $\sin(\lambda_{03}y)$, and $\sin(\lambda_{10}x)\sin(\lambda_{01}y)$ on both sides of these two equations within the accuracy of $O(\varepsilon)$, and eliminating a_{ij} from the resulting equations, one can obtain

$$\left. \begin{aligned} \ddot{b}_{10} + 2\zeta_{10}\dot{b}_{10} + b_{10} + H_1(b_{10}, b_{01}, b_{20}, b_{11}) &= -\psi_{10}r_{10}\ddot{x}_g \cos \alpha \\ \ddot{b}_{01} + 2\zeta_{01}\omega_{01}\dot{b}_{01} + \omega_{01}^2 b_{01} + H_2(b_{10}, b_{01}, b_{02}, b_{11}) &= -\psi_{01}r_{01}\ddot{x}_g \sin \alpha \\ \ddot{b}_{20} + 2\zeta_{20}\omega_{20}\dot{b}_{20} + \omega_{20}^2 b_{20} + H_3(b_{10}, b_{01}, b_{30}) &= 0 \\ \ddot{b}_{02} + 2\zeta_{02}\omega_{02}\dot{b}_{02} + \omega_{02}^2 b_{02} + H_4(b_{10}, b_{01}, b_{03}) &= 0 \\ \ddot{b}_{30} + 2\zeta_{30}\omega_{30}\dot{b}_{30} + \omega_{30}^2 b_{30} + H_5(b_{10}, b_{01}, b_{20}) &= -\psi_{30}r_{30}\ddot{x}_g \cos \alpha \\ \ddot{b}_{03} + 2\zeta_{03}\omega_{03}\dot{b}_{03} + \omega_{03}^2 b_{03} + H_6(b_{10}, b_{01}, b_{02}) &= -\psi_{03}r_{03}\ddot{x}_g \sin \alpha \\ \ddot{b}_{11} + 2\zeta_{11}\omega_{11}\dot{b}_{11} + \omega_{11}^2 b_{11} + H_7(b_{10}, b_{01}) &= 0 \end{aligned} \right\} \quad (13)$$

where $\omega_{ij}^2 = \psi_{ij}/\psi_{10}$ and $\psi_{ij} = \lambda_{ij} \tanh(\lambda_{ij}h)$. Note that linear viscous damping terms $2\zeta_{ij}\omega_{ij}\dot{b}_{ij}$ are incorporated in Eq. (13) to consider the damping effect of sloshing. The nonlinear terms H_m ($m=1, 2, \dots, 7$) in Eq. (13) are:

$$\left. \begin{aligned} H_1 &= S_1\dot{b}_{10}\dot{b}_{20} + S_2\dot{b}_{01}\dot{b}_{11} + S_3\dot{b}_{10}^2 b_{10} + S_4\dot{b}_{01}^2 b_{10} + S_5\dot{b}_{10}\dot{b}_{01}b_{01} \\ &\quad + S_6b_{10}b_{20} + S_7b_{01}b_{11} + S_8b_{10}^3 + S_9b_{01}^2 b_{10} \\ H_2 &= S_{10}\dot{b}_{01}\dot{b}_{02} + S_{11}\dot{b}_{10}\dot{b}_{11} + S_{12}\dot{b}_{01}^2 b_{01} + S_{13}\dot{b}_{10}^2 b_{01} \\ &\quad + S_{14}\dot{b}_{10}\dot{b}_{01}b_{10} + S_{15}b_{01}b_{02} + S_{16}b_{10}b_{11} + S_{17}b_{01}^3 + S_{18}b_{10}^2 b_{01} \\ H_3 &= S_{19}b_{10}^2 + S_{20}\dot{b}_{10}\dot{b}_{30} + S_{21}b_{10}^2 + S_{22}b_{10}b_{30} \\ H_4 &= S_{23}\dot{b}_{01}^2 + S_{24}\dot{b}_{01}\dot{b}_{03} + S_{25}b_{01}^2 + S_{26}b_{01}b_{03} \\ H_5 &= S_{27}\dot{b}_{10}\dot{b}_{20} + S_{28}\dot{b}_{10}^2 b_{10} + S_{29}b_{10}b_{20} + S_{30}b_{10}^3 \\ H_6 &= S_{31}\dot{b}_{01}\dot{b}_{02} + S_{32}\dot{b}_{01}^2 b_{01} + S_{33}b_{01}b_{02} + S_{34}b_{01}^3 \\ H_7 &= S_{35}\dot{b}_{10}\dot{b}_{01} + S_{36}b_{10}b_{01}, \end{aligned} \right\} \quad (14)$$

where the symbols S_n ($n=1, 2, \dots, 36$) are constants defined by the system parameters and their perfect expressions are omitted here. Because the nonlinear terms of b_{10} and b_{01} are included in H_1 and H_2 of Eq. (14), (1,0) and (0,1) modes are nonlinearly coupled and form an autoparametric system.

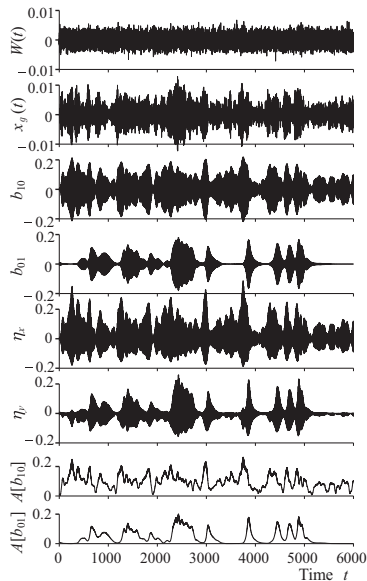


Fig. 3. Time histories when $h=0.6$, $w=1.0$, $\zeta_{ij}=0.013$, $\alpha=0^\circ$, $\gamma=0.03$, $S_0=1.0 \times 10^{-7}$ and $\Omega=0.98$.

3 Numerical results

Figure 3 shows the time histories from the Monte Carlo simulation. The values of the parameters are $h=0.6$, $w=1.0$, $\zeta_{ij}=0.013$, $\alpha=0^\circ$, $\gamma=0.03$, $S_0=1.0 \times 10^{-7}$ and $\Omega=0.98$. The Runge-Kutta-Gill method is used to conduct the numerical simulation. The time step of the simulation is set as $\Delta t=0.25$, hence the Nyquist frequency $\omega_N=2\pi/(2\Delta t)=\pi/\Delta t=12.57$. η_x and η_y represent the liquid elevations at positions $(x,y)=(0.5,0)$ and $(0,0.5)$, respectively, as shown in figure 1. $A[b_{10}]$ and $A[b_{01}]$ represent the amplitudes of b_{10} and b_{01} , respectively, and are calculated by

$$A[b_{10}] = \sqrt{b_{10}^2 + (\dot{b}_{10}/\Omega)^2}, \quad A[b_{01}] = \sqrt{b_{01}^2 + (\dot{b}_{01}/\Omega)^2}. \quad (15)$$

Because (1,0) mode is directly excited, b_{10} and η_x oscillate violently. Furthermore (0,1) mode is indirectly excited because the two modes are nonlinear coupled and b_{01} and η_y intermittently oscillate. This is known as ‘‘autoparametric interaction.’’

3.1. Influence of Bandwidth

Figures 4(a) and 4(b) show the simulation results of the mean square responses of (1,0) and (0,1) sloshing modes, respectively. The values of the parameters are the same as those in figure 3. The mean square values $E[b_{10}^2]$ and $E[b_{01}^2]$ are plotted by \bullet and $E[\eta_x^2]$ and $E[\eta_y^2]$ are plotted by \circ . These values are estimated from the time histories during $t=1000-6000$ using 100 different sets of random number series. The dash-dotted line represents the theoretical curves for the corresponding linear sloshing model. In figures 4(a) and 4(b) simulation results deviate significantly from the theoretical curves near $\Omega=1.0$. This is due to the autoparametric interaction. The values of $E[b_{10}^2]$ on the left hand side of $\Omega=1.0$ are larger which correspond to a soft nonlinear Duffing oscillator under harmonic excitation. Because \circ includes higher sloshing modes, it appears at slightly higher values than \bullet .

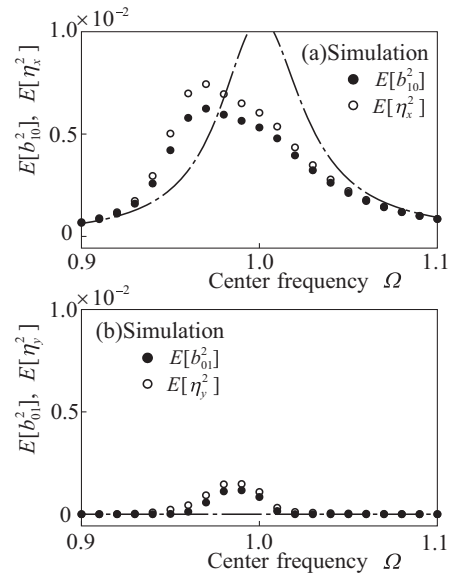


Fig. 4. Mean square responses including the results of Fig. 3.

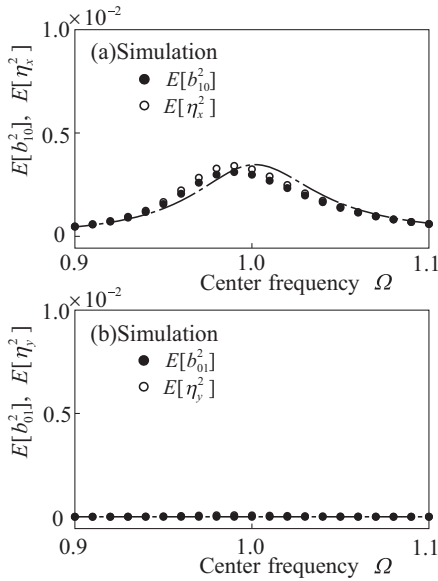


Fig. 5. Same as figure 4, but $\gamma=0.06$.

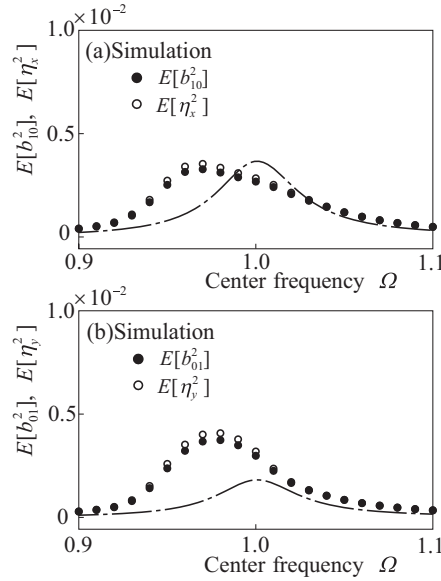


Fig. 6. Same as figure 4, but $\alpha=40^\circ$.

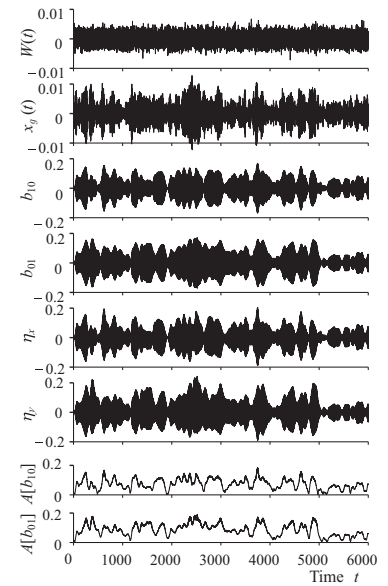


Fig. 7. Time histories at $\Omega=0.98$ in Fig. 6.

Figure 5 shows the simulation results of the mean square responses when only the value of the bandwidth is changed from $\gamma=0.03$ in figure 4 to 0.06. As γ increases, the mean square response $E[b_{10}^2]$ flattens and the simulation results are closer to the theoretical curve. This implies that the interaction between (1, 0) and (0, 1) modes is not as significant. Further increasing the bandwidth would probably result in a flat line.

3.2 Influence of Excitation Direction

Figure 6 shows the influence of the excitation direction on the mean square responses when only the value of α is changed from $\alpha=0^\circ$ in figure 4 to 40° . When $\alpha=40^\circ$, (1, 0) and (0, 1) sloshing modes are both directly excited by random ground excitation and the theoretical curve of $E[b_{10}^2]$ for the linear sloshing model is larger than that of $E[b_{01}^2]$. However, the simulation results are opposite on the left hand side of $\Omega=1.0$.

Figure 7 shows the time histories at $\Omega=0.98$ in figure 6. It can be seen that b_{01} oscillates at higher amplitudes than b_{10} . When the value of α increases from 0° to 45° , even though (1, 0) mode receives more energy from the ground excitation, its mean square value $E[b_{10}^2]$ is not usually larger than that of (0, 1) mode. When the bandwidth is narrow, this result is similar to that of a system under harmonic excitation, where multi-valued response curves are observed [6].

4 Conclusions

The mean square responses of the predominant sloshing modes in a square tank have been investigated when subjected to horizontal, narrow-band random ground excitation. The results are summarized as follows:

1. When the bandwidth is narrow and $\alpha=0^\circ$, autoparametric interaction occurs and the mean square responses of (1, 0) mode under direct excitation are

decreased by the occurrence of (0, 1) mode depending on the center frequency.

2. Increasing the bandwidth results in less autoparametric interaction and flatter simulation results of the mean square responses.

3. When $0^\circ < \alpha < 45^\circ$, although both modes are directly excited, (1, 0) mode receives more energy from the ground excitation. However, its mean square values are not usually larger than those of (0, 1) mode.

For further work, the influence of the intensity of random ground excitation and liquid level should be investigated as well as the risk of overspill, most likely at two opposing corners of the tank.

References

1. G.W. Housner, Bull. Seismic Soc. Am. **47**, 15-35 (1957)
2. R.A. Ibrahim, *Liquid Sloshing Dynamics*, (Cambridge University Press, Cambridge, UK, 2005)
3. R.E., Hutton, NASA Technical Note D-1870, 1-64 (1963)
4. H.N. Abramson, NASA SP-106 (1966)
5. O.M. Faltinsen, O.F. Rognebakke, A.N. Timokha, J. Fluid Mech. **487**, 1-42 (2003)
6. T. Ikeda, R.A. Ibrahim, *Proc. the 22nd Interl. Cong. of Theoretical and Appl. Mech.* (ICTAM2008), Adelaide, Australia, August 24-29 (2008)
7. M. Sakata, K. Kimura, M. Utsumi, J. Sound Vib. **94**(3), 351-363 (1984)
8. C.Z. Wang, B.C. Khoo, F, Ocean Engineering **32**(2), 107-133 (2005)
9. A. Soundrarajan, R.A. Ibrahim, J. Sound Vib. **121**(3), 445-462 (1988)
10. T. Ikeda, R.A. Ibrahim, J. Sound Vib. **284**(1-2), 75-102 (2005)
11. T. Ikeda, ASME, J. Comput. Nonlinear Dyn. **6**(2), #021001 (2011)